

# Efficient step-mediated intercalation of silver atoms deposited on the $\text{Bi}_2\text{Se}_3$ surface

M. M. Otkrov<sup>\*1)</sup>, S. D. Borisova<sup>\*+</sup>, V. Chis<sup>×</sup>, M. G. Vergniory<sup>×°</sup>, S. V. Eremeev<sup>\*+</sup>, V. M. Kuznetsov<sup>\*</sup>,  
E. V. Chulkov<sup>×∇</sup>

<sup>\*</sup>*Tomsk State University, 634050 Tomsk, Russia*

<sup>+</sup>*Institute of Strength Physics and Materials Science SB of the RAS, 634021 Tomsk, Russia*

<sup>×</sup>*Donostia International Physics Center (DIPC), 20018 San Sebastián/Donostia, Basque Country, Spain*

<sup>°</sup>*Max-Planck-Institut für Mikrostrukturphysik, D-06120 Halle, Germany*

<sup>∇</sup>*Departamento de Física de Materiales UPV/EHU and Centro de Física de Materiales CFM and Centro Mixto CSIC-UPV/EHU, 20080 San Sebastián/Donostia, Basque Country, Spain*

Submitted 2 October 2012

The intercalation of silver atoms into the van der Waals gap of the prototypical three-dimensional topological insulator  $\text{Bi}_2\text{Se}_3$  is studied by means of *ab initio* total-energy calculations. Two possible intercalation mechanisms are examined: penetration from the terrace under the step and penetration via interstitials and/or vacancies of the surface quintuple layer block. It is shown that the former mechanism is strongly preferred over the latter one due to significant energy gain appearing at the step. According to performed estimations, the room temperature diffusion length of silver atoms reaches ten microns within a couple of minutes both on the surface and within the van der Waals gap, which essentially exceeds a typical distance between steps. These results shed light on the mechanism of intercalation of metal atoms deposited on the  $\text{Bi}_2\text{Se}_3$  surface.

Topological insulators are of significant interest currently due to their unique transport properties and potentially important technological applications [1, 2]. A great effort has been undertaken in order to find or engineer the topological insulator materials with suitable properties [3–12]. Among known topological insulators,  $\text{Bi}_2\text{Se}_3$  has gained a foothold as a most promising one due to a large bulk band gap and ideal Dirac cone [13, 14].

The evolution of electronic and structural properties of topological insulator surfaces upon deposition of various adsorbates is of special interest. Typically, the Dirac state survives upon such an adsorption, however, additional Rashba-split two-dimensional electron gas states arise at the surface, as was shown for  $\text{Bi}_2\text{Se}_3$  and  $\text{Bi}_2\text{Te}_3$  exposed to molecules [15–18], alkali [17, 19–21], noble [21–23], and magnetic [21, 24–26] metal atoms. Meanwhile, structural investigations of the impurity-deposited  $\text{Bi}_2\text{Se}_3$  surface revealed partial [20] or almost complete [22, 23] disappearance of adatoms at room and higher temperatures. The authors of these works claimed that majority of the adatoms intercalates below the surface, presumably into the van der Waals (vdW) gaps of the  $\text{Bi}_2\text{Se}_3$  crystal, however the mechanism of such an intercalation has not been investigated yet. To

study this mechanism we consider the case of the silver atoms deposited on the surface of the prototypical three-dimensional topological insulator  $\text{Bi}_2\text{Se}_3$ . Using *ab initio* total-energy calculations, we show that the Ag atoms penetrate into the vdW gap mostly from the terrace under the step. Moreover, the room temperature diffusion length of the Ag adatoms both on the surface and within the vdW gap was found to reach ten microns within a couple of minutes.

The crystal structure of  $\text{Bi}_2\text{Se}_3$  is formed by quintuple layer (QL) blocks separated by the vdW gaps, in each QL the hexagonal atomic planes follow the order Se–Bi–Se–Bi–Se (Fig. 1a). Being equal to 2.54 Å, the vdW gaps in  $\text{Bi}_2\text{Se}_3$  are 0.64–0.95 Å greater than interlayer distances inside the QL, thus representing a natural place for intercalation. While the bonding between atoms belonging to the same QL is of covalent-ionic type, neighboring QLs are only weakly vdW bonded. Therefore the adjacent QL blocks can be considered as almost independent in the sense that processes taking place on the surface QL or in between two QLs don't affect much the underlying QL or the nearest ones. For this reason, in the present work the study of diffusion on the surface was performed using a slab of 5 atomic layers (i.e. 1 QL), while for the study of diffusion within the vdW gap a slab of 10 atomic layers (2 QLs) was constructed. In both cases the isolated silver atoms were considered us-

<sup>1)</sup>otrovov@phys.tsu.ru

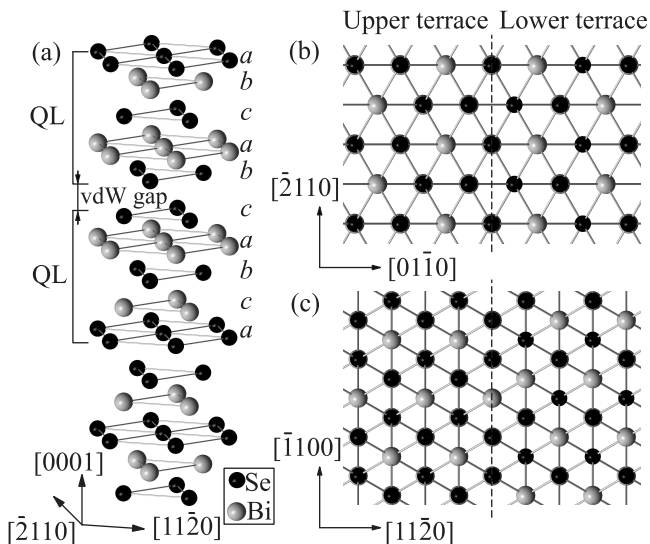


Fig. 1. (a) – Crystal structure of  $\text{Bi}_2\text{Se}_3$ ,  $abc$  is the atomic layer stacking sequence. (b), (c) – Top views of the  $\text{Bi}_2\text{Se}_3$  surface containing  $[01\bar{1}0]$ -oriented (b) and  $[11\bar{2}0]$ -oriented (c) steps. The steps are marked by dashed lines

ing  $3 \times 3$  in-plane cells. The behavior of the Ag adatom in the vicinity of  $[01\bar{1}0]$ -oriented ( $[11\bar{2}0]$ -oriented) step was studied using supercell containing one full  $3 \times 6$  ( $2\sqrt{3} \times 6$ ) QL and  $3 \times 3$  ( $2\sqrt{3} \times 3$ ) step-terminated QL on top of it (Fig. 1b and c).

For DFT calculations we employed the projector augmented-wave method [27] in VASP implementation [28, 29]. The generalized-gradient approximation was used to describe the exchange-correlation potential [30] and the spin-orbit coupling was neglected. In order to correctly account for the vdW interactions we made use of DFT-D2 approach proposed by Grimme [31]. More specifically, this approach was utilized for the study of silver diffusion both inside the vdW gap and on top of the surface where the vdW interactions are important. As far as the diffusion through the QL is concerned, the vdW interactions were neglected because of the chemical nature of bonding inside QL.

We start from the fact that, regardless of the intercalation mechanism itself, the energy gain arising upon relocation of a single Ag atom from the surface to the vdW gap is equal to 0.267 eV. The question about the intercalation mechanism then arises. The total-energy calculations, performed under assumption that the silver atoms penetrate into the vdW gap via interstitials of QL, yield migration barrier value of the order of 1.4 eV. Note, that similar value ( $\sim 1$  eV) was obtained for the copper adatom barrier in Ref. [22]. Since the value of the barrier is quite high such a mechanism can hardly be responsible for disappearance of deposited adatoms from the surface.

Obviously, the intercalation is mediated by defects of the crystal structure.  $\text{Bi}_2\text{Se}_3$  is known to demonstrate two kinds of point defects, the antisite defects (i.e. Bi atom occupies Se position) and selenium vacancies [32, 33]. The former can hardly make intercalation easier, in contrast to the latter, which can provide a channel for intercalation. We found that the silver atom readily occupies the topmost layer Se vacancy and gains an energy of 0.26 eV with respect to that of neighboring fcc hollow site (which is the most energetically favorable position for the isolated silver atom on the surface, see positions 9, 11, 13, and 15 in Fig. 2). However, since further motion of the adatom is restricted solely to the interstitial regions, the “global” barrier doesn’t change much from that of the case of defectless QL, i.e. it is still of the order of 1.4 eV. The presence of the third-layer Se vacancies can also be suggested. Our calculations show that if the Ag atom successfully overcomes a barrier of 0.64 eV upon passing through the subsurface Bi layer, then it occupies the third-layer Se vacancy and gains an energy of 0.87 eV with respect to that at the surface. This means that the third-layer Se vacancy acts as a trap for the silver atom: once this vacancy is reached the atom would have difficulties abandoning it, because the energy of  $\sim 1.5$  eV is needed to go back to the surface or towards the vdW gap. According to Refs. [22, 34], the areal density of Se vacancies at the  $\text{Bi}_2\text{Se}_3$  surface amounts of a minimum of  $\sim (1 \pm 0.2) \cdot 10^{11} \text{ cm}^{-2}$ . Meanwhile, in Ref. [23] the silver coverage used was equal to 0.4 monolayer, which corresponds to  $\sim 2.7 \cdot 10^{14} \text{ cm}^{-2}$ . It is evident therefore, that saturation of the third-layer Se vacancies cannot explain disappearance of 0.4 monolayer of deposited Ag within several minutes, as it was observed in Ref. [23]. We also checked the migration barriers in the presence of Bi vacancies (which are in fact very rare in  $\text{Bi}_2\text{Se}_3$  material) and found that significant decrease of the barrier (from 1.4 to 0.55 eV) appears only in the case of two nearest Bi vacancies situated in different layers. These results show that in fact very few silver atoms can penetrate through the topmost QL and reach the vdW gap.

Other defects which can assist the intercalation are steps, arising at the  $\text{Bi}_2\text{Se}_3$  surface upon cleavage or during epitaxial growth [22, 34, 35]. A big length of steps, around several hundreds of nanometers, may favor simultaneous penetration of many adatoms in the vdW gaps. However, the distances between neighboring steps reach 100 nm and in order to achieve the step the adatom diffusion length must be greater than 100 nm. The problem of determination of the diffusion length  $l = \sqrt{zDt}$  ( $t$  is time,  $D = D_0(\nu_0) \exp(-E_m/k_B T)$  is a diffusion coefficient and  $z$  is a number of places to jump to) traces

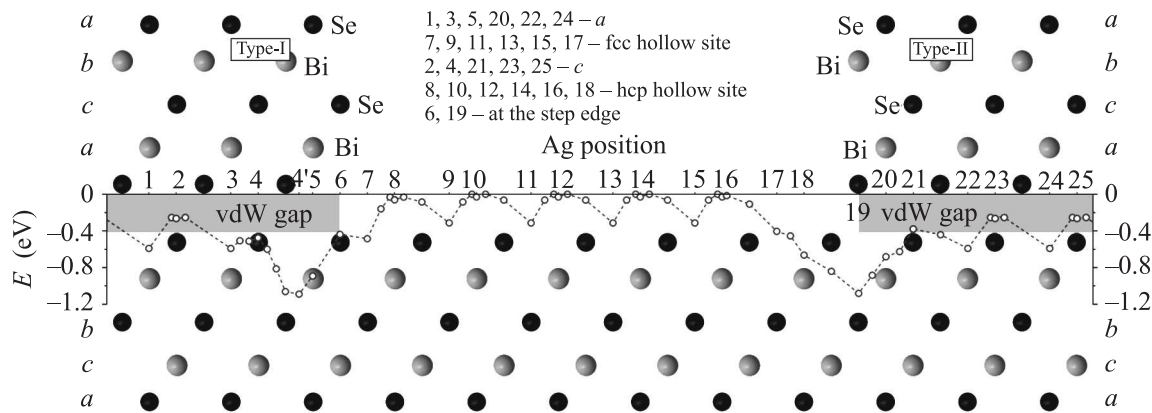


Fig. 2. The total energy as a function of the silver atom position on the surface, in the vicinity of the  $[01\bar{1}0]$ -oriented step and inside the vdW gap. Two different terminations of  $[01\bar{1}0]$ -oriented step are shown: type-I (left) and type-II (right)

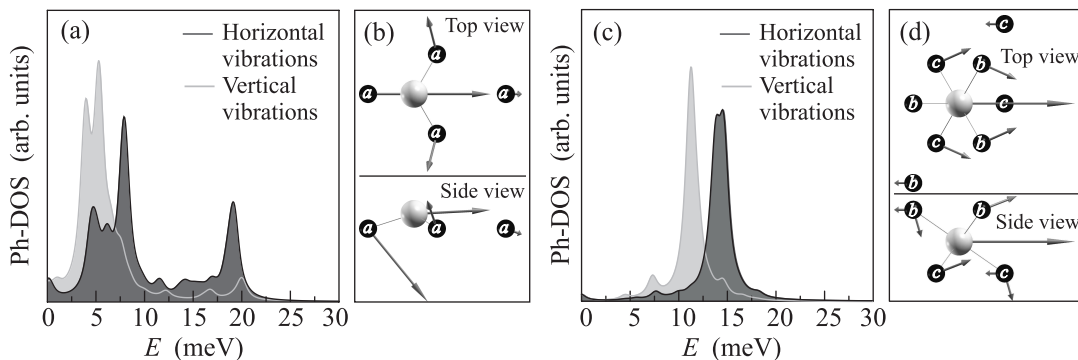


Fig. 3. (a), (c) – Ph-DOS projected onto the Ag atom placed at the fcc hollow site on the  $\text{Bi}_2\text{Se}_3$  surface (a) or within the vdW gap in  $a$  position (c). The lines with dark and light gray shading correspond to the horizontal and vertical components, respectively. (b), (d) – Displacement fields corresponding to the vibrational modes which facilitate the Ag atom jump from one fcc hollow site to another one (b) and from  $a$  position to  $c$  position in the vdW gap (d). Big light ball denotes the silver atom. On (b) only underlying Se layer is shown, while on (d) only Se layers adjacent to the vdW gap are shown: upper –  $b$ , lower –  $c$

back to the estimation of the minimal migration barriers  $E_m$  and adatom vibrational frequencies  $\nu_0$ . According to our total-energy calculations, the easiest way to travel over the surface is hopping between neighboring fcc hollow sites along the  $\text{fcc} \rightarrow \text{bridge} \rightarrow \text{hcp} \rightarrow \text{bridge} \rightarrow \text{fcc}$  curved path over the energy barriers of  $0.314 \text{ eV}$ , see Fig. 2. The latter are shifted from the hcp hollow sites (positions 8, 10, 12, 14, and 16 on Fig. 2) towards neighboring bridge sites by  $a_0/(6\sqrt{3})$ , where  $a_0$  is the  $\text{Bi}_2\text{Se}_3$  in-plane lattice parameter. The vibrational frequencies  $\nu_0$  were calculated by applying density functional perturbation theory (DFPT) as implemented in the Quantum ESPRESSO package [36]. In Fig. 3a we present the phonon density of states (Ph-DOS) projected onto the Ag atom situated at the fcc hollow site on the  $\text{Bi}_2\text{Se}_3$  surface. The vibrational modes which facilitate the Ag atom jump from one fcc hollow site to another one contribute to the Ph-DOS peak with maximum at  $7.82 \text{ meV}$  ( $1.89 \text{ THz}$ ). Fig. 3b shows representative displacement

field of these modes: one can see that Se atoms enclosing bridge position move apart thus making Ag atom easier to jump in between. Knowing  $E_m$  and  $\nu_0$ , one can calculate the diffusion length  $l$ . The prefactor  $D_0$  is defined as  $\frac{1}{z}\nu_0 a_0^2$ , where  $a_0$  is a jump length which in our case is equal to the in-plane lattice parameter and  $z = 6$  is a number of neighboring fcc hollow positions. Calculated dependencies of the diffusion length and the diffusion coefficient on temperature are shown in Fig. 4. It can be seen that at  $100 \text{ K}$  the motion of the adatoms is frozen because  $l$  is extremely small, of the order of  $10^{-5} \mu\text{m}$  within  $1 \text{ s}$  time window. At approximately  $210 \text{ K}$  the diffusion length becomes comparable with a typical distance between neighboring steps at the  $\text{Bi}_2\text{Se}_3$  surface ( $\sim 0.1 \mu\text{m}$  [22, 34, 35]), and finally, at  $300 \text{ K}$ , the diffusion length exceeds  $1 \mu\text{m}$ . These results signify that silver atoms can cover distances of the order of ten microns within couple of minutes, and thus are able to reach the steps. Note, that our results also

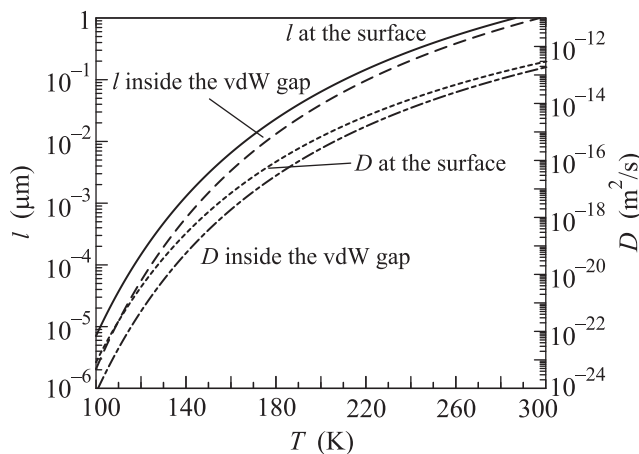


Fig. 4. The temperature dependencies of the diffusion length,  $l$  (left axis), and the diffusion coefficient,  $D$  (right axis), of the silver atom on the  $\text{Bi}_2\text{Se}_3$  surface and within the vdW gap estimated within 1 s time window. Both dependencies drawn in logarithmic scale. The temperature range is chosen in accordance with those in available experimental works [22, 23]

correlate with those obtained experimentally for the copper adsorbates deposited on the  $\text{Bi}_2\text{Se}_3$  surface [22]: at 100 K the  $\text{Bi}_2\text{Se}_3$  surface is covered by a small Cu clusters, whereas at 300 K scanning tunneling microscopy measurements show almost clean  $\text{Bi}_2\text{Se}_3$  surface. Besides, the values of diffusion coefficients obtained in our work are in good agreement with theoretically estimated values for the copper atoms on  $\text{Bi}_2\text{Se}_3$  [22].

Let us now analyze the migration barriers in the vicinity of the step. There are two possible orientations of the steps on the  $\text{Bi}_2\text{Se}_3$  surface: step perpendicular to the  $[01\bar{1}0]$  direction (Fig. 1b) and step perpendicular to the  $[11\bar{2}0]$  direction (Fig. 1c). Fig. 2 shows energy profile for the motion of the silver atom towards the  $[01\bar{1}0]$ -oriented step for two terminations of the latter. Once the step is reached, the Ag atom readily enters the vdW gap lowering the total energy by approximately 0.78 eV with respect to that of the fcc hollow site at the surface. Herewith, in order to jump back to the terrace the diffusant must overcome a barrier of the order of 1.1 eV for both type-I and type-II termination cases. However, to move further within the vdW gap, the Ag atom has to climb a significantly lower barrier, 0.61 eV (0.7 eV) for type-I (type-II) termination. As far as  $[11\bar{2}0]$ -oriented step is concerned, the energy profile for the adatom motion towards the step is similar (not shown). The system gains energy of 0.744 eV when the adatom reaches a step, but after that it has to overcome an energy barrier of 0.752 eV to diffuse further within the vdW gap. The estimation of the time needed to pass over this barrier

will be made below. Note, that in order to move back to the terrace an energy of 1.06 eV is required.

The scanning tunneling microscopy measurements [23] performed for the Ag-intercalated  $\text{Bi}_2\text{Se}_3$  surface revealed protrusions with lateral size of 3 nm whose formation was explained by presence of intercalated Ag atoms inside the vdW gap. Obviously, protrusions of such sizes cannot be due to isolated atoms and rather caused by the Ag clusters. This means that Ag atoms must be able to freely travel within the vdW gap in order to aggregate and form clusters or, in other words, the room temperature diffusion length in the vdW gap must be comparable to that at the surface. Our total-energy calculations indicate the  $a$  position as a most stable one for an Ag atom inside the vdW gap (positions 1, 3, 22, and 24 in Fig. 2). The energy cost for migration of a silver atom in the vdW gap is moderate: it has to overcome a barrier of 0.34 eV in case if diffusion occurs between  $a$  and  $c$  sites (positions 2, 23, and 25 in Fig. 2; like at the surface, the barrier point is shifted from the symmetric position), while a slightly higher barrier of 0.38 eV arises along the  $a \rightarrow a$  path (not shown). To estimate vibrational frequency we again resort to DFPT. In Fig. 3d we show a typical displacement field of modes ( $\sim 14$  meV, i.e. 3.36 THz, see Fig. 3c) which facilitate the Ag atom jump towards the  $c$  position, i.e. in the direction of minimal barrier. Note, that the expression for  $D_0$  is again  $\frac{1}{6}\nu_0 a_0^2$ , since for each  $a$  site there are six positions to jump to: three  $c$  sites and three  $b$  sites, which are equivalent to  $c$  ones. As a result of the diffusion length estimations the picture similar to that obtained for the surface diffusion arises: the motion of the Ag atoms is frozen at 100 K, however at 300 K they can cover distances of the order of  $10 \mu\text{m}$  within a couple of minutes.

Thus, we have shown that silver atoms are able to freely travel over the  $\text{Bi}_2\text{Se}_3$  surface and within the vdW gap at room and higher temperatures. However one important question still should be answered: are the silver atoms able to overcome the energy barriers of 0.61–0.752 eV arising just after the step threshold? To answer this question one needs to estimate the vibrational frequencies of the atoms in the positions with minimal energies at the step (positions 4' and 19 for  $[01\bar{1}0]$  step, see Fig. 2). Performing DFPT calculations in this case would require a vast computational effort. Let us notice, however, that vibrational frequencies for the adatom on the surface and within the vdW gap have the same order. Therefore a rough estimation can be made by interpolating between these two situations. Thus, one may choose  $\nu_0$  value of 2.64 THz. Evaluating the time which is needed for a silver atom at 300 K to overcome the en-

ergy barrier of 0.61 eV (0.7 eV) under the  $[01\bar{1}0]$  step and reach nearest  $a$  position one gets a value of 6.7 ms (0.22 s), while for the  $[11\bar{2}0]$  step with the barrier of 0.752 eV this time is 1.63 s. One can conclude that  $[01\bar{1}0]$  steps should provide substantially faster intercalation of the silver atoms into the vdW gaps.

These results indicate that the step-mediated intercalation of the Ag atoms into the  $\text{Bi}_2\text{Se}_3$  vdW gap is strongly preferred over the intercalation through the surface QL. As discussed above, the estimated diffusion coefficients for the migration of the Ag atom on the surface and within the vdW gap are in good agreement with those obtained for the Cu atom in work [22]. Thus, one can expect that revealed step-mediated intercalation mechanism may be universal for metal atoms deposited on the  $\text{Bi}_2\text{Se}_3$  or another layered topological insulator surface.

In conclusion, intercalation of silver atoms deposited on the  $\text{Bi}_2\text{Se}_3$  surface was studied within DFT. We have shown that the intercalation is step-mediated in the sense that the Ag atoms penetrate into the vdW gap when they achieve the step on the surface. The factors responsible for the high efficiency of step-mediated intercalation are big diffusion length of the silver atoms both on the surface and within the vdW gap and significant energy gain appearing at the step. At the same time, penetration via interstitials and/or vacancies of the topmost QL is less probable due to high energy barriers. These results provide an explanation of the intercalation mechanism of metal atoms deposited on the  $\text{Bi}_2\text{Se}_3$  surface.

We acknowledge partial support from the University of the Basque Country (Grant #GIC07IT36607) and the Spanish Ministerio de Ciencia e Innovación (Grant #FIS2010-19609-C02-00). Calculations were performed on SKIF-Cyberia supercomputer of Tomsk State University.

---

1. M. Z. Hasan and C. L. Kane, *Rev. Mod. Phys.* **82**, 3045 (2010).
2. X.-L. Qi and S.-C. Zhang, *Rev. Mod. Phys.* **83**, 1057 (2011).
3. Y. L. Chen, J. G. Analytis, J.-H. Chu et al., *Science* **325**, 178 (2009).
4. D. Hsieh, Y. Xia, D. Qian et al., *Phys. Rev. Lett.* **103**, 146401 (2009).
5. B. Yan, C.-X. Liu, H.-J. Zhang et al., *Europhys. Lett.* **90**, 37002 (2010).
6. S. V. Eremeev, Yu. M. Koroteev, and E. V. Chulkov, *JETP Lett.* **91**, 594 (2010).
7. T. Sato, K. Segawa, H. Guo et al., *Phys. Rev. Lett.* **105**, 136802 (2010).

8. K. Kuroda, M. Ye, A. Kimura et al., *Phys. Rev. Lett.* **105**, 146801 (2010).
9. T. V. Menshchikova, S. V. Eremeev, Yu. M. Koroteev et al., *JETP Lett.* **93**, 15 (2011).
10. S. V. Eremeev, G. Landolt, T. V. Menshchikova et al., *Nature Commun.* **3**, 635 (2012).
11. K. Kuroda, H. Miyahara, M. Ye et al., *Phys. Rev. Lett.* **108**, 206803 (2012).
12. I. V. Silkin, T. V. Menshchikova, M. M. Otrokov et al., *Pis'ma v ZhETF* **96**, 352 (2012).
13. Y. Xia, D. Qian, D. Hsieh, et al., *Nature Phys.* **5**, 398 (2009).
14. H. Zhang, C.-X. Liu, X.-L. Qi et al., *Nature Phys.* **5**, 438 (2009).
15. M. Bianchi, R. C. Hatch, J. Mi et al., *Phys. Rev. Lett.* **107**, 086802 (2011).
16. H. M. Benia, C. Lin, K. Kern et al., *Phys. Rev. Lett.* **107**, 177602 (2011).
17. P. D. C. King, R. C. Hatch, M. Bianchi et al., *Phys. Rev. Lett.* **107**, 096802 (2011).
18. C. Chen, S. He, H. Weng et al., *Proceedings of the National Academy of Sciences* **109**, 3694 (2012).
19. Z.-H. Zhu, G. Levy, B. Ludbrook et al., *Phys. Rev. Lett.* **107**, 186405 (2011).
20. M. Bianchi, R. C. Hatch, Z. Li et al., *ACS Nano* **6**, 7009 (2012).
21. T. Valla, Z.-H. Pan, D. Gardner et al., *Phys. Rev. Lett.* **108**, 117601 (2012).
22. Y.-L. Wang, Y. Xu, Y.-P. Jiang et al., *Phys. Rev. B* **84**, 075335 (2011).
23. M. Ye, S. V. Eremeev, K. Kuroda et al., arXiv:1112.5869 (2011).
24. M. Ye, S. V. Eremeev, K. Kuroda et al., *Phys. Rev. B* **85**, 205317 (2012).
25. J. Honolka, A. A. Khajetoorians, V. Sessi et al., *Phys. Rev. Lett.* **108**, 256811 (2012).
26. M. R. Scholz, J. Sánchez-Barriga, D. Marchenko et al., *Phys. Rev. Lett.* **108**, 256810 (2012).
27. P. E. Blöchl, *Phys. Rev. B* **50**, 17953 (1994).
28. G. Kresse and J. Furthmüller, *Phys. Rev. B* **54**, 11169 (1996).
29. G. Kresse and J. Joubert, *Phys. Rev. B* **59**, 1758 (1999).
30. J. P. Perdew, K. Burke, and M. Ernzerhof, *Phys. Rev. Lett.* **77**, 3865 (1996).
31. S. Grimme, *J. Comp. Chem.* **27**, 1787 (2006).
32. J. Horák, Z. Stary, P. Lošt'ák et al., *J. Phys. Chem. Solids* **51**, 1353 (1990).
33. Y. S. Hor, A. Richardella, P. Roushan et al., *Phys. Rev. B* **79**, 195208 (2009).
34. C.-L. Song, Y.-L. Wang, Y.-P. Jiang et al., *Appl. Phys. Lett.* **97**, 143118 (2010).
35. P. Cheng, C. Song, T. Zhang et al., *Phys. Rev. Lett.* **105**, 076801 (2010).
36. P. Giannozzi, S. Baroni, N. Bonini et al., *J. Phys. Cond. Mat.* **21**, 395502 (2009).